Time-lapse 3D VSP using permanent receivers in a flowing well in the deepwater Gulf of Mexico

Han Wu, Denis Kiyashchenko, and Jorge Lopez, Shell International Exploration and Production

The vision of smart wells permanently instrumented with geophones has existed for some time. Such installations would enable opportunities for frequent reservoir monitoring, high-resolution 3D VSP imaging, and illumination of difficult areas. For many subsalt fields, 3D VSPs acquired in such wells may be the best option to illuminate and monitor reservoirs without the need to stop production or enter a well. However, this technology is not yet widely applied, nor perhaps proven.

As part of the OBS (ocean-bottom survey) 4D seismic program in the Mars Field in the deepwater Gulf of Mexico, we got the opportunity to evaluate these concepts. Our study area is a narrow region around the Mars TLP (tension leg platform) between two salt bodies. Twelve fiber-optic vertical-component borehole seismic receivers were permanently installed in 2006 in one production well at a spacing of 75 ft and ranging from 13,057 to 13,882 ft in depth. This is the first deepwater deployment of the Weatherford Clarion system (the first offshore installation was done in Valhall Field of the North Sea, see Hornby et al., 2007). The two 3D VSP data sets were recorded simultaneously with the 2007 and 2010 OBS acquisitions, allowing us to get 3D VSP shots "for free." During the recording, the well was in full production.

The installation, acquisition, and possibility to create an image out of the 2007 baseline data were reported by Hornby and Burch (2008). Our paper outlines the data issues and results of time-lapse processing of these surveys. We came across two major challenges during data processing. First, the acquisition of the 3D VSP monitor survey was limited due to logistical and operational issues. Second, the data had poor signal-to-noise ratio (SNR) due to production noise, tube waves, and fiber-optic receiver sensitivity. Therefore, special care had to be taken for noise removal during both baseline and monitor data processing. Time-lapse processing required regularization of the data to the same shot grid and matching of the first-arrival waveforms. As the result, we obtained a baseline 3D VSP image that ties the OBS seismic image, has higher resolution, and gives better illumination in the areas close to salt. In the time-lapse sense, the images are fairly repeatable in the areas of high fold around the receiver well. This shows that the permanent in-well fiber-optic receiver installation can be used for reservoir monitoring. Such a solution is an attractive option for subsalt field development when the optimal illumination of the producing targets requires a 3D VSP geometry.

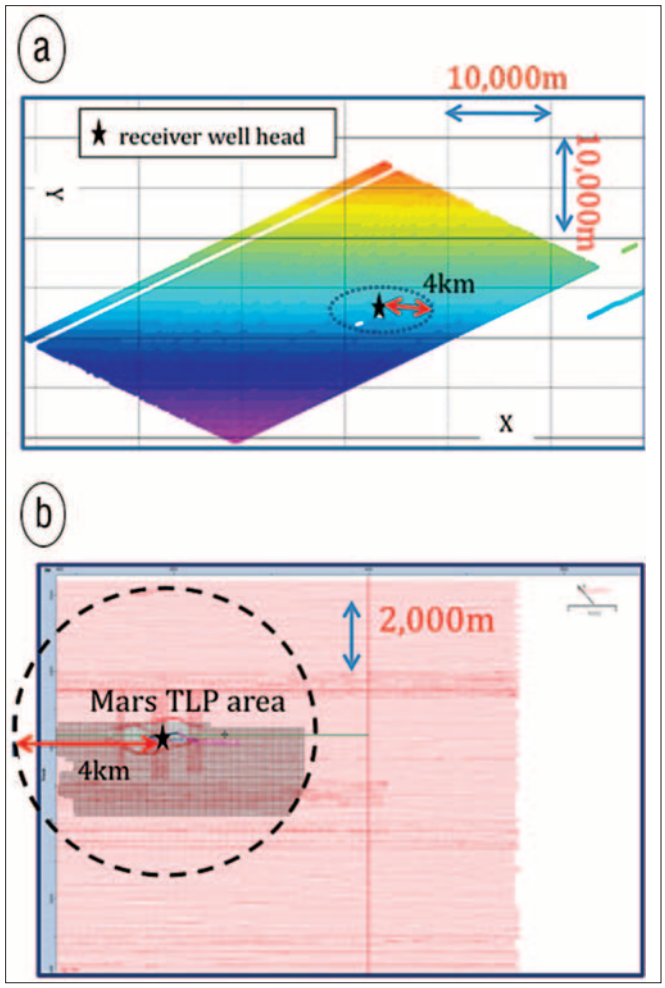

Figure 1. *(a) The OBS survey shot map. The circle of 4-km radius outlines shots used in processing. Star denotes the receiver well head. (b) Zoom of the area around Mars TLP. Black shows 3D VSP baseline shots used in processing of monitor survey (see Figure 4). Nominal shot spacing is 50 m in inline (SW-NE direction) and 40 m in crossline shooting directions.*

The baseline 2007 3D VSP: Processing issues and results

The permanent VSP receivers recording OBS shots give us an opportunity to have a very large number of shots (160,000) potentially leading to high fold and wide coverage. In order to illustrate the extent of the survey, the OBS shot map is shown in Figure 1a. The radius of the small circle around the production well is about the receiver tool depth (4 km). For usual 3D VSP design, shot offsets would not usually exceed that distance from a receiver well. Recording of large-offset shots would be useful when imaging dipping structures. The zoomed area around Mars TLP (Figure 1b) shows very dense shot coverage (nominally 50-m spacing in inline shooting direction and 40-m spacing in crossline shooting direction). However, the raw data were significantly contaminated by different kinds of noises. Figure 2a shows an example of several shot gathers of the 2007 3D VSP data recorded on the 12 vertical component receivers. The strongest events visible are tube waves. They are characterized by constant moveout

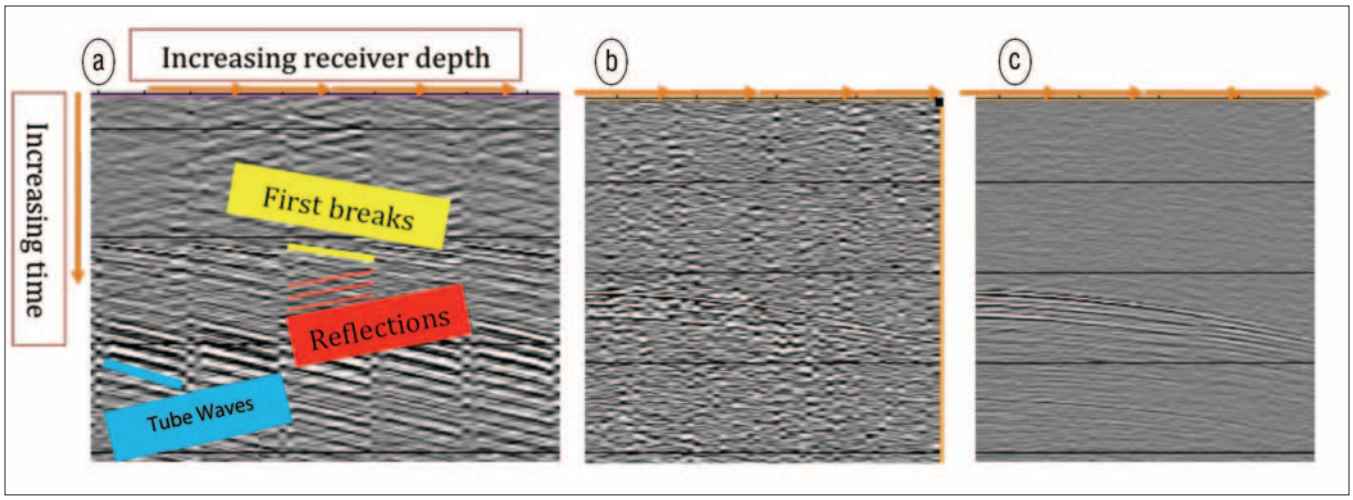

Figure 2. *(a) Example of a near-offset shot gather recorded on the 12 vertical component fiber-optic receivers shows that reflections are obscured by strong tube waves. (b) Example of receiver gather (13,400 ft receiver depth). (c) The receiver gather after noise suppression exhibits much improved SNR.*

for all the survey. The direct arrivals are also visible, but the upgoing reflection energy is quite difficult to notice. Besides the noise caused by coherent tube waves, there was a lot of incoherent noise, apparently caused by sensitivity of fiber-optic recording to the environment (see the receiver gather example in Figure 2b). Due to signal-to-noise issues, we limited the shots used for processing to a maximal offset of 4.3 km (i.e., shot gathers inside the circle in Figure 1, which have visible first arrivals)—a total of approximately 25,000 shots.

Tube waves were quite easy to remove, given their constant moveout, by applying a median filter in the common-shot domain. The up-down wavefield separation was also done with a median filter. To make incoherent noises sparser, the upgoing waves were sorted to the receiver domain. The receiver gather has a multiplicity of the number of shots (~25,000 after shot selection for the baseline data) that is much larger than the multiplicity of the shot gather (number of receivers—12), which allows us to remove sparsely distributed, high-amplitude, low-frequency noise. Next, the source locations were regularized to a grid of 50 × 40 m (the nominal shot grid). Finally, the signal was boosted by removing the incoherent noises with a least-squares type filter (see Canales, 1984) in the receiver domain (Figure 2c). A reverse time migration (RTM) was used to generate the final depth image. The anisotropic velocity model derived from the baseline OBS data (other seismic surveys and well data were used as well) by Stopin et al. (2008) was used for migration.

Figure 3b shows the 3D VSP image overlaid on the 2007 OBS image (Figure 3a, see Stopin et al., 2008). The VSP events tie the OBS interpreted horizons in both dip direction and event spacing. Advantages of the VSP image are its higher frequency (see spectral comparison in Figure 3c), and better illumination in the updip direction toward the salt, where the OBS image is dim.

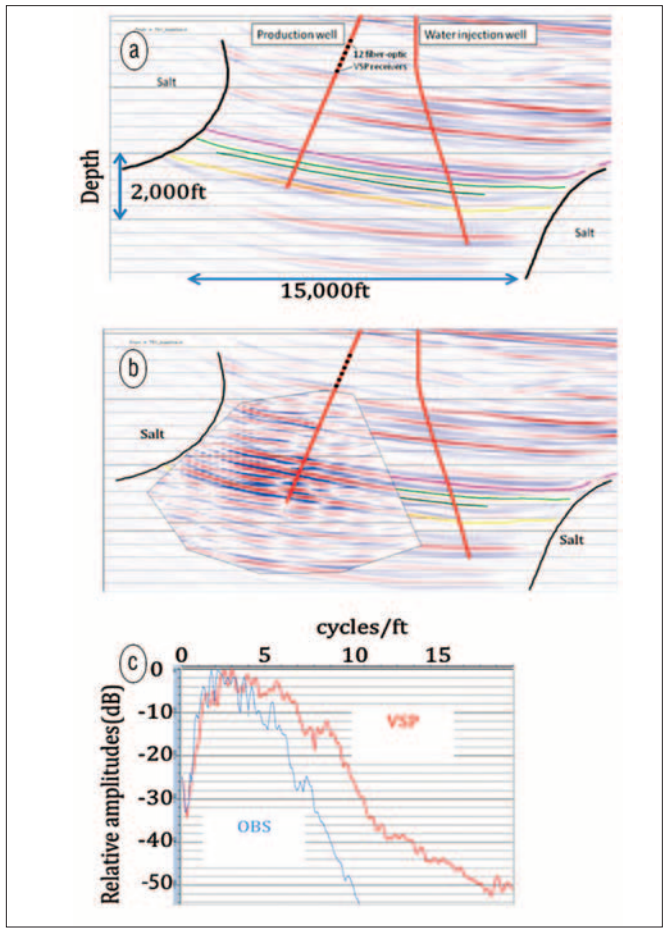

Figure 3. *2007 3D VSP image compared with 2007 OBS image. (a) 2007 OBS image around the VSP study area. The black dots on the production well path show the location of the 12 fiber-optic receivers. The paths of the production well and water injection well are also shown. (b) 2007 3D VSP image overlaid on the 2007 OBS image showing good tie to OBS image, but better illumination toward the salt (the conflicting flat dips are imaging artifacts). (c) Spectral comparison demonstrating higher frequency content of the VSP image.*

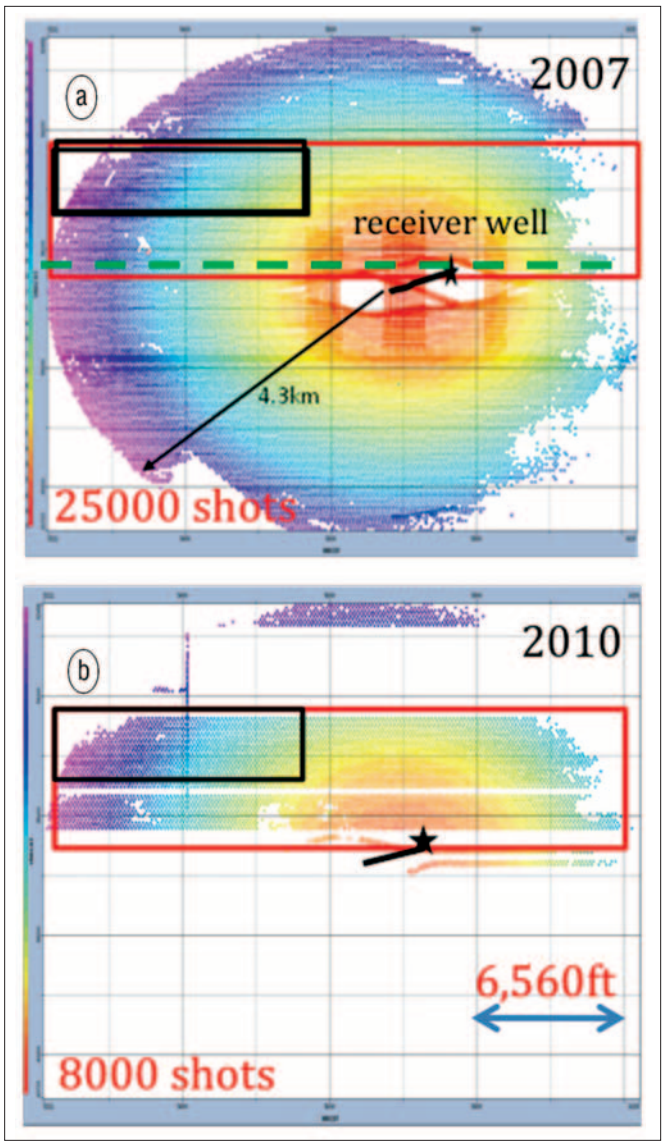

Figure 4. *Map of baseline (a) and monitor (b) shots with visible first arrivals. The black star shows the production well location. The black line shows the production well path. The permanent receivers were installed near the TD (total depth) of this well. The red box indicates the common shot area between baseline and monitor surveys much reduced because of issues while recording the VSP shots in 2010. The shots in the black box were excluded from final migration. The green dashed line indicates the traverse for image displays in Figures 5–7.*

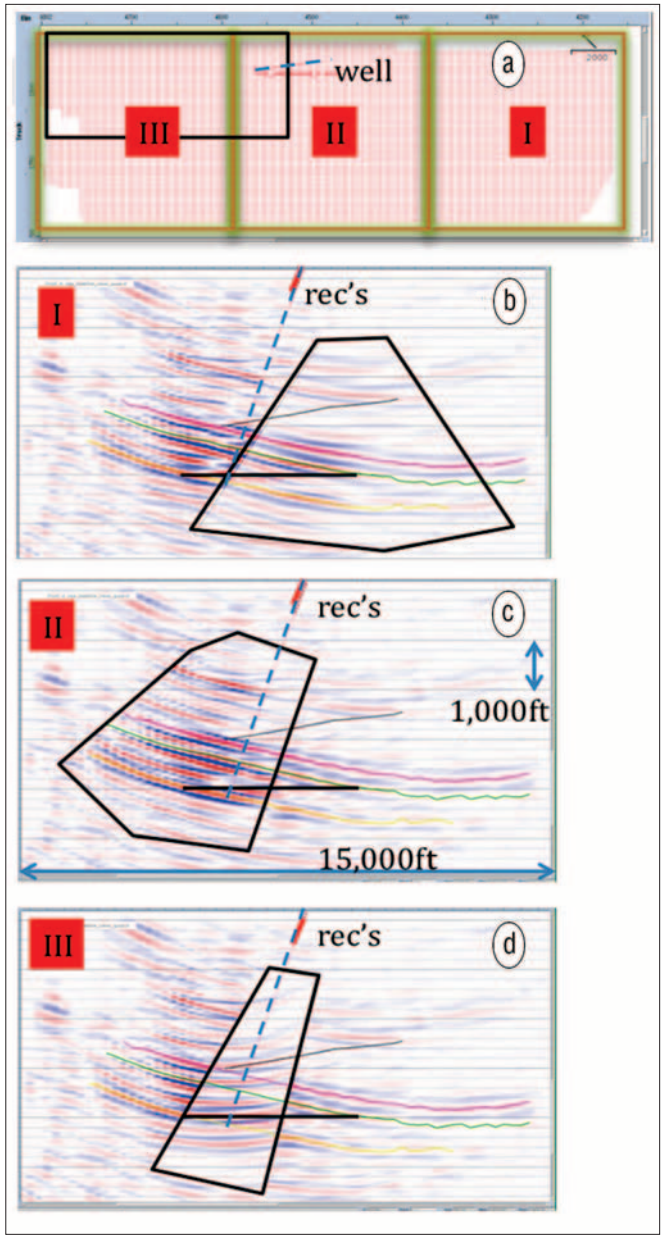

Figure 5. *(a) The strip of shots split into three groups (I, II, III). (b) Migration of group I shots (black box) spliced into the image obtained with all shots. Black line corresponds to conflicting dips. (c) Migration of group II shots. (d) Migration of group III shots. We see that conflicting dips result from migration of group III shots. Ray tracing shows that shots within black box in (a) ultimately produce the flat-dip artifacts.*

Time-lapse processing of the 2007 and 2010 3D VSPs

The key components of 4D VSP processing are regularization and matching. Regularization produces the same shot geometry for baseline (2007 VSP) and monitor (2010 VSP). It provides a grid base for 3D matching. Matching reduces source wavelet amplitude and phase differences between baseline and monitor data sets. Downhole VSP recording allows us to use downgoing waves (not influenced by reservoir changes below the receivers) to derive matching filters.

Figure 4 shows a map of baseline (a) and monitor (b) shots with visible first arrivals (distributed inside a circle of 4.3-km radius around the well). The red box outlines the area where the monitor shots overlapped with the baseline shots. To be clear, the 2010 OBS shots overlapped the 2007 OBS shots fully (about 160,000 shots), and we were able to use a subset of these shots (25,000 inside a 4.3-km radius from the wellhead) for baseline 3D VSP processing. Unfortunately, due to logistical and operational issues, only about 8000 usable shots (falling within a 4.3-km radius) were acquired downhole during the 2010 OBS survey (Figure 4b). The baseline and monitor shots inside the red box are regularized to the same grid before up-down separation.

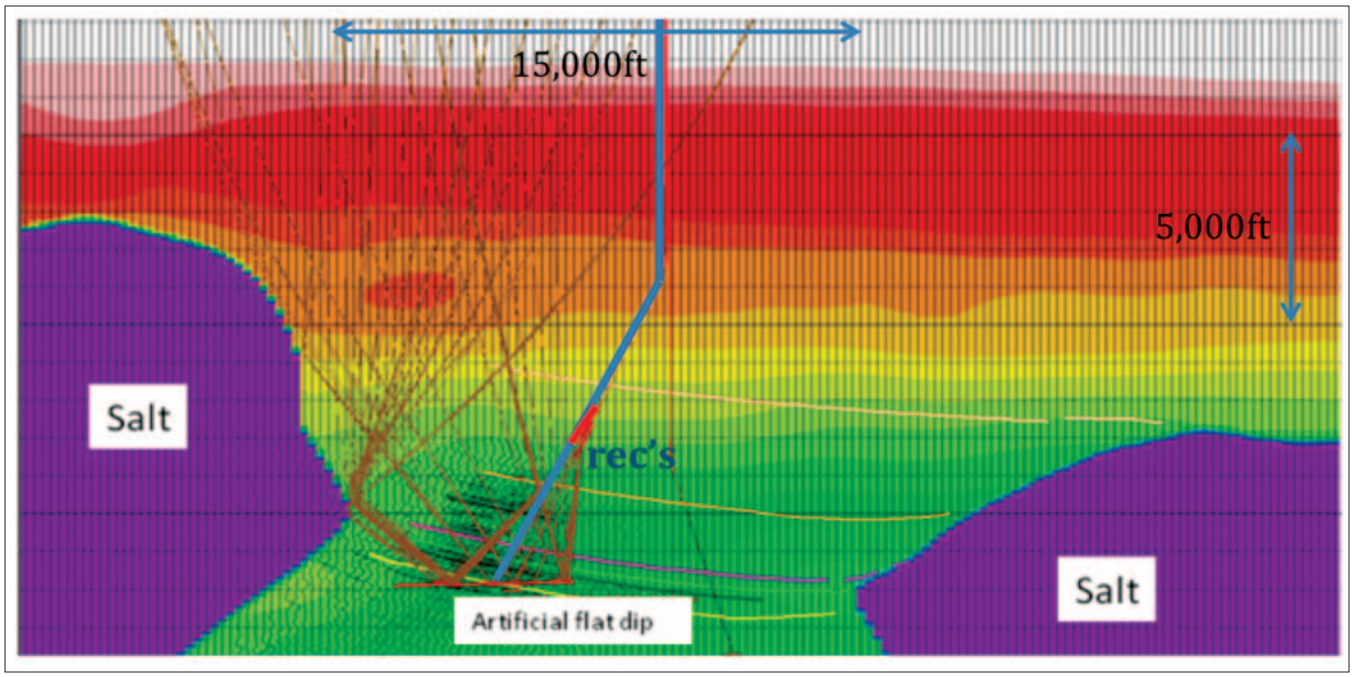

Figure 6. *Two-point ray tracing with a source at one VSP receiver and the artificial flat dip as a reflector shows a second reflection from the salt. Most of the surface exit points from these double reflections are distributed inside the black box in Figures 4 and 5.*

Matching is applied to reduce the differences in the source wavelets between the baseline and monitor upgoing waves. For each trace, a short window around the first breaks (excluding useful reflections) is used to derive the optimal Wiener-type matching filter. This filter is then applied to the whole trace length of the baseline data. Three types of differences have been observed between baseline and monitor first breaks: time differences (few milliseconds), phase differences (up to 30°), and amplitude differences. Possible reasons for having these differences are water velocity changes and different air-gun depths between 2007 and 2010 surveys. Matching on the first break removes any 4D effect above the receivers, but preserves 4D effects in the region below the receivers that is illuminated by reflected waves.

Before migration of regularized and matched baseline and monitor data, it was desirable to find the origin of the conflicting flat dips in the area around the producing well (see Figure 3b). For that purpose, the data were migrated separately for three shot groups (Figure 5) along the strip of collocated shots (red box in Figure 4). The conflicting dips were caused by the shots in the third group (Figure 5d). To locate the problematic shots more precisely, the conflicting dip artifacts were picked on the final image (black lines in Figure 5) and reflections from them were traced to the surface. The exit points were located within the black box in Figure 5a. As illustrated by the two-point ray tracing in Figure 6, shot points inside the black box contributed to the artificial flat dips in the migrated image (Figure 3b) through a second reflection from the salt. The reflections from deeper horizons might be migrated along these raypaths, thus producing con-

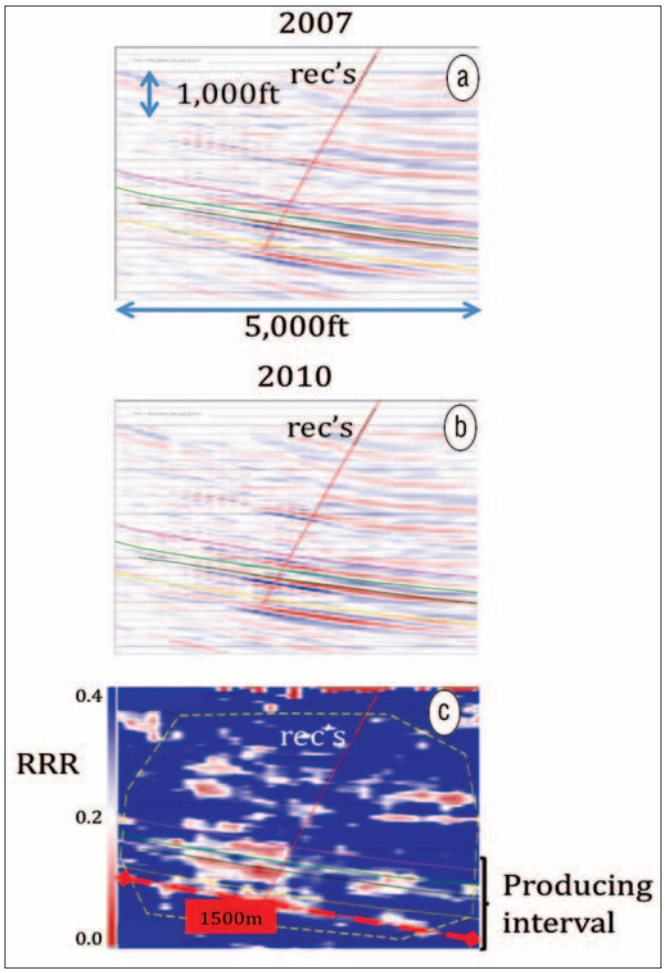

Figure 7. *4D processing results and repeatability. (a) Baseline 3D VSP image. (b) Monitor 3D VSP image. (c) The rms repeatability ratio (RRR) attribute section. Smaller RRR values correspond to better repeatability (red and white). Yellow dashed polygon delineates the zone with good repeatability, which has a width of 1500 m around the VSP well. In the producing interval, RRR is around 0.06.*

flicting dips in the image. The matched baseline and monitor data were supplied to the final migration excluding the shots outlined by the black box in Figure 4. Excluding these shots from migration improves the event continuity and, hence, 4D repeatability.

The 3D VSP surveys did not illuminate sufficiently the downdip area around the injector well (Figure 3) to see reliable time-lapse changes where they were expected. However, it was possible to assess the repeatability of such an OBS-VSP data set. The repeatability analysis is important because it allows us to estimate how strong the time-lapse signal should be in order to be detected. The baseline and monitor images for the traverse in Figure 4 are shown in Figure 7a and 7b. The same velocity model was used for baseline and monitor migrations. For repeatability analysis we use the rms repeatability ratio (RRR) attribute defined as:

$$RRR = \frac{2RMS(\mathbf{a}-\mathbf{b})}{RMS(\mathbf{a})+RMS(\mathbf{b})};\ RMS(\mathbf{a}) = \sqrt{\frac{1}{N}\sum_{i=1}^{N} a_i^{\,2}}$$

for baseline data record **a** and monitor data record **b** with rms(**a**) being the root mean square amplitude of the record **a**. The RRR attribute multiplied by 100% is widely known as nrms or normalized root mean square of the difference between baseline and monitor data (Kragh and Christie, 2002). This attribute was computed for each image trace in a running window of 130 depth samples (about 500 m). In order to avoid time-lapse artifacts due to depth shifts of monitor image with respect to baseline image, prior to RRR calculation the events in monitor image were shifted in depth to maximize their correlation with baseline events. Figure 7c shows the RRR section along the same traverse. The red and white areas correspond to good image repeatability. Blue areas correspond to reduced repeatability which is typical for image areas without any prominent events. The time-lapse noise amplitudes divided by small amplitudes of seismic events lead to increased RRR. The events above the producing interval have small amplitude and there are a lot of reduced repeatability areas. We have the majority of representative events in the producing interval. Although the areas of reduced repeatability are present there too, within an inline distance of 750 m at each side of the well, the average RRR value is around 0.2. It means that the rms amplitude of time-lapse noise is about 20% of the signal amplitude. This value is comparable to repeatability estimates for conventional marine time-lapse seismic surveys (Smit et al., 2005). RRR near strong events in the 3D VSP image is often equal to 0.06 or less. This is a very good value for 4D VSP, especially given the low data quality and small channel number.

Conclusions and outlook

We have demonstrated that data recorded on permanently installed fiber-optic borehole seismic sensors can be processed and validated against surface seismic when careful attention is paid to noise removal and first break picking. A better image is achieved in the updip area of the target reservoir section where surface seismic is dim. Higher frequency gives more detail within the reservoir section.

Our time-lapse analysis shows that in the region surrounding the receivers, the repeatability characterized by RRR of 0.2 (nrms of 20%) is achieved within a range of 1500 m around the VSP well and even lower around strong events within the producing interval. This is a very good value considering the low data quality and low fold of this VSP data set (12 receivers). It is indeed comparable to repeatability of marine seismic time-lapse surveys which are widely used nowadays.

Generally, the impact of low SNR on the data should be clearly understood and weighted against the expected 4D signal. On the acquisition side, it will be useful to develop and deploy permanent receivers that have better SNR characteristics than the ones used here. Otherwise, production shut-in should be considered as an option for low SNR risk mitigation. Development of longer arrays will also be essential for improvement, as well as their placement in wells that illuminate the area of interest.

It is remarkable that a 3D VSP image may be obtained in such challenging environment of a short borehole array re-

cording data in a well under full production (see also Hornby and Burch, 2008). It is even more remarkable that a 4D signal may be extracted in such noisy environment. Our results provide significant encouragement to the vision of a dual OBS- or OBC-VSP monitoring system (OBC stands for ocean-bottom cable), where the 4D effects measured on the ocean bottom survey may be complemented and calibrated by the downhole sensors. The downhole acquisition itself is essentially free, as it records shots "paid by" the seabed survey on receivers permanently installed without need to enter a well or stop production. Using a dual permanent system (OBC, VSP) has the added benefit of reduced acquisition costs. Both permanent systems, on the seabed and downhole, will incur large upfront capital investments, to be amortized over the life of the field. This proposition becomes especially attractive when surveys are repeated often or on demand. Such systems may provide the only viable and cost-effective solution to monitor fields under salt. TLE

References

Canales, L., 1984, Random noise reduction: 54th Annual International Meeting, SEG, Expanded Abstracts, 525–527.

Hornby, B., O. Barkved, O. Askim, F. Bostick, and B. Williams, 2007, Permanent fiber-optic borehole seismic installation and imaging at Valhall: 69th EAGE Conference and Exhibition.

Hornby, B. and T. Burch, 2008, Passive "drive by" imaging in a deep water production well using permanent borehole seismic sensors: 78th Annual International Meeting, SEG, Expanded Abstracts, 349–352.

Kragh, E. and P. Christie, 2002, Seismic repeatability, normalized RMS, and predictability: The Leading Edge, **27**, no. 7, 640–647, doi:10.1190/1.1497316.

Smit, F., J. Brain, and K. Watt, 2005, Repeatability monitoring during marine 4D streamer acquisition: 67th EAGE Conference and Exhibition.

Stopin, A., M. Mc Rae, L. Lepre, and B. Gaudin, 2008, Constructing an anisotropic velocity model for ocean-bottom seismic node data: 78th Annual International Meeting, SEG, Expanded Abstracts, 993–997.

Acknowledgments: We are grateful to Paul Hatchell for his interpretation insights and suggestion to run migration tests, Alexandre Stopin for discussions about water velocity statics, Gerard Soto and Yingping Li for preparing the raw data and providing the acquisition information for us; Bill Butler for his help in ray-tracing; and Dharmpal Takhar for deriving debubble filters. We are grateful to our partner BP for initial data processing and QC. In particular, we appreciate the efforts of our BP colleagues Brian Hornby and Tom Burch who initiated the data acquisition and analysis. We are thankful to Reinaldo Michelena and Colin MacBeth for their comments and suggestions for paper improvement. We thank Shell and BP for permission to publish this paper.

Corresponding author: Denis.Kiyashchenko@shell.com